Supporting Information

Associations of interannual and interdecadal variation of Summer Tropospheric Ozone with Western Pacific Subtropical High in China

By Zhang et al.

SI Text 1. Model evaluation

Extensive model evaluations were performed by comparing simulated ozone concentrations with monitored data collected from China's Environmental Monitoring Center (CNENC, http://106.37.208.233:20035/). The CNEMC started operation in 2013 and provides hourly monitored tropospheric ozone concentrations across China from 2013 onward. Considering large uncertainties of sampled ambient air quality data in the first several years, we collected monitoring data in summer 2016 to verify modeled O_3 concentrations. We compared six hourly modeled and measured O_3 concentrations. **Figure S1a-S1f** show the modeled and sampled six-hourly O_3 concentrations in six UAs in summer 2016. The modeled O_3 concentrations capture, to a large extent, the fluctuations of measured concentrations with the correlation coefficients $R > 0.6$ ($p<0.01$), except for CC at $R=0.56$. **Figure S1g** is a correlation diagram between the modeled and measured six-hourly (0200, 0800, 1400, 2000 LST) O_3 concentrations in six UAs from June 1st to August 31st, 2016. Although there are some deviations from the 1:1 line between modeled and measured O_3 concentrations, the fraction of the modeled values is mostly within a factor of two of measured O_3 (FA2) with a correlation coefficient of 0.71 ($p<0.01$, $n=2190$).

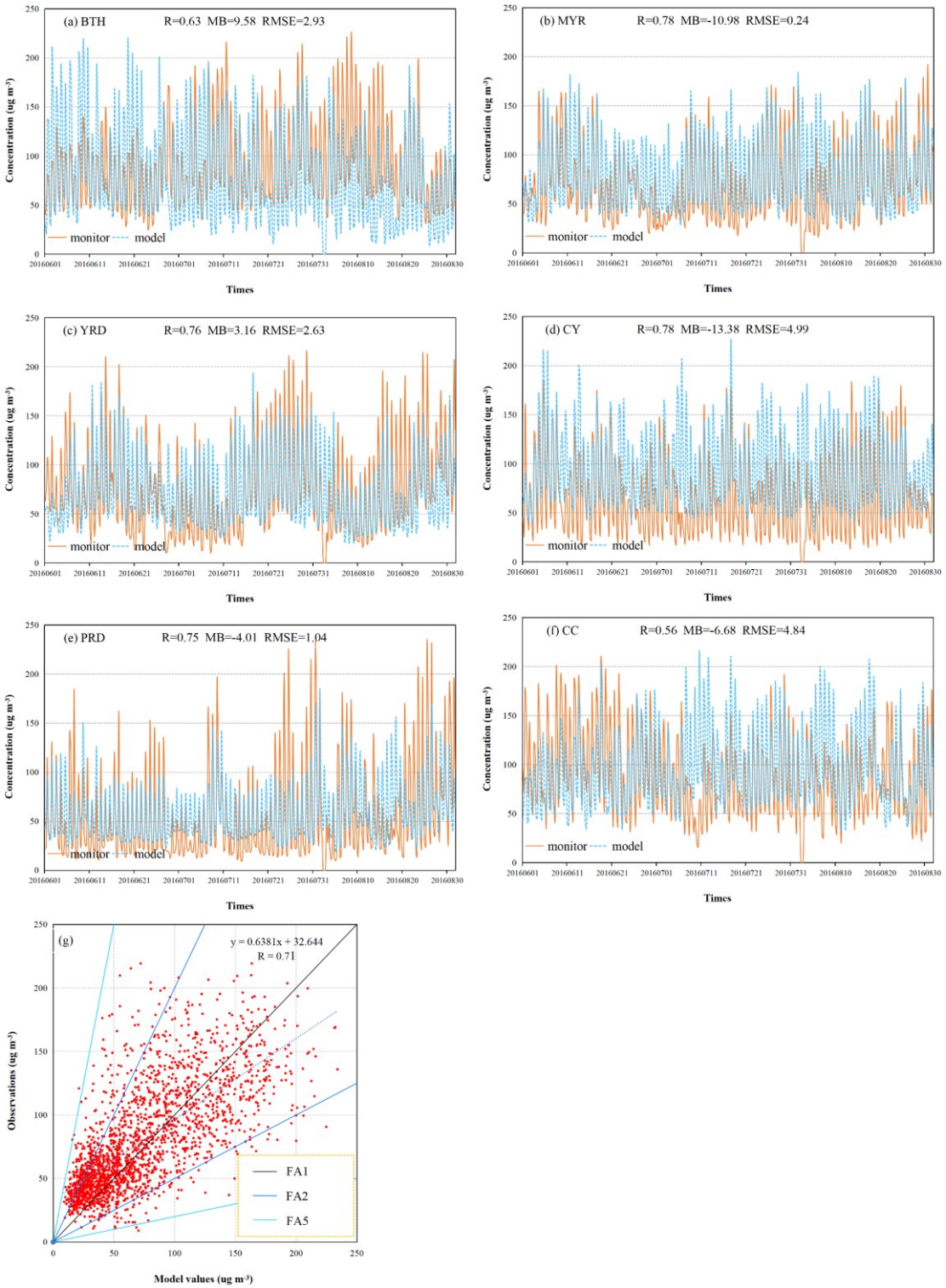

Figure S1. (**a-f**) Monitored (solid orange line) and modeled (dashed blue line) six hourly O_3 concentrations in six UAs in summer 2016; (**g**) A correlation diagram between modeled and measured six hourly (0200, 0800, 1400, 2000 LST) O_3 concentrations in six UAs from June 1st to August 31st 2016. The number of total samples is 2190. R is correlation coefficient. FA1, FA2, and FA5 are the fractions of model values within factors of one to five of measure O_3 concentrations.

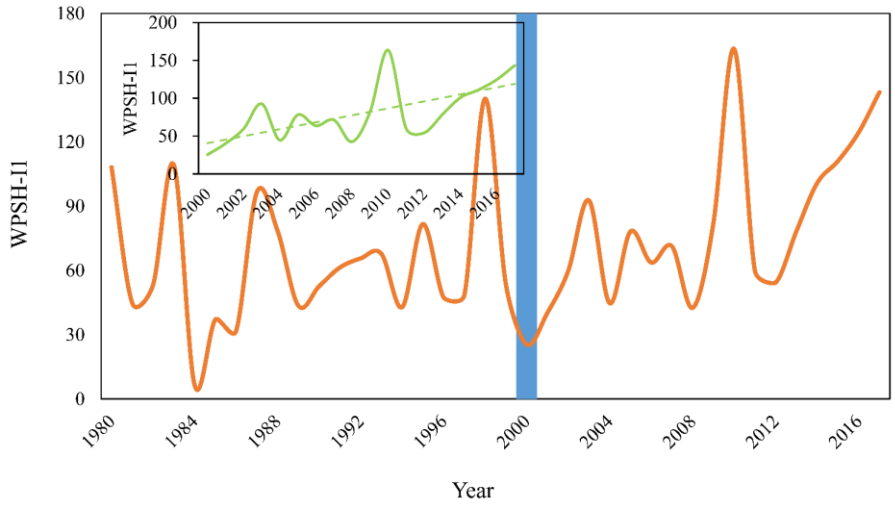

Figure S2. Summer WPSH-I1 from 1980 to 2017. The inset figure on the top-left shows summer WPSH-I1 from 2000 to 2017 and its trend (dashed green line). Blue shading indicates 2000.

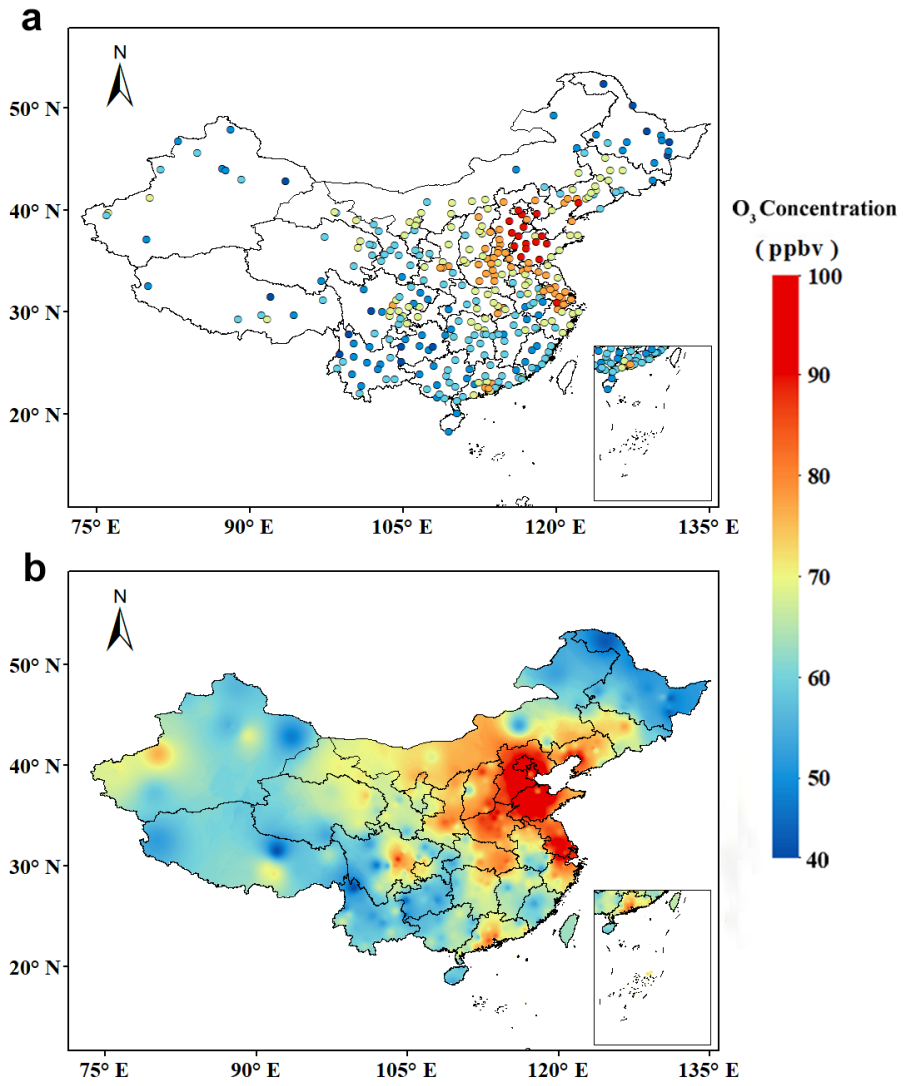

Figure S3. Measured summer O_3 concentrations (ppbv) averaged from 2015 to 2017 across China. (a) Sampled summer O_3 concentrations; (b) interpolated summer O_3 levels.

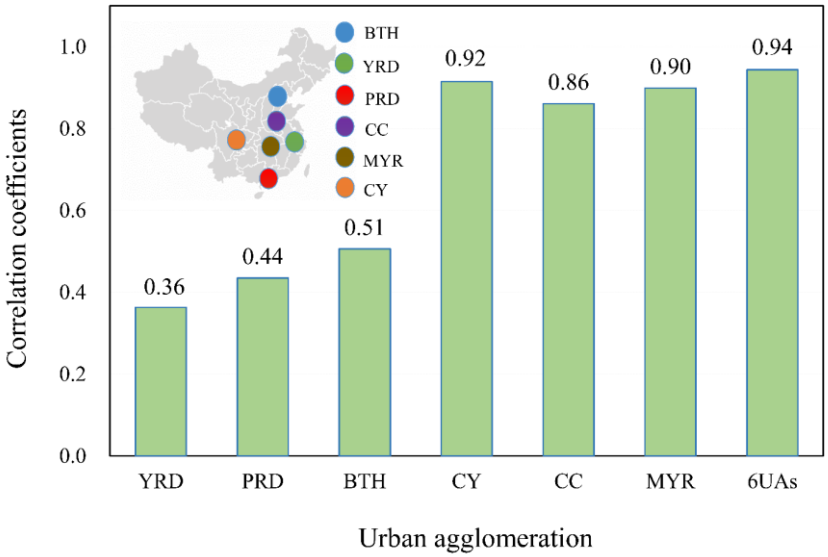

Figure S4. Correlation coefficients between the first EOF loading and summer O_3 concentrations in each UA and averaged over the six UAs from 1999 to 2017. Inner figure on the upper left shows locations of six UAs in China.

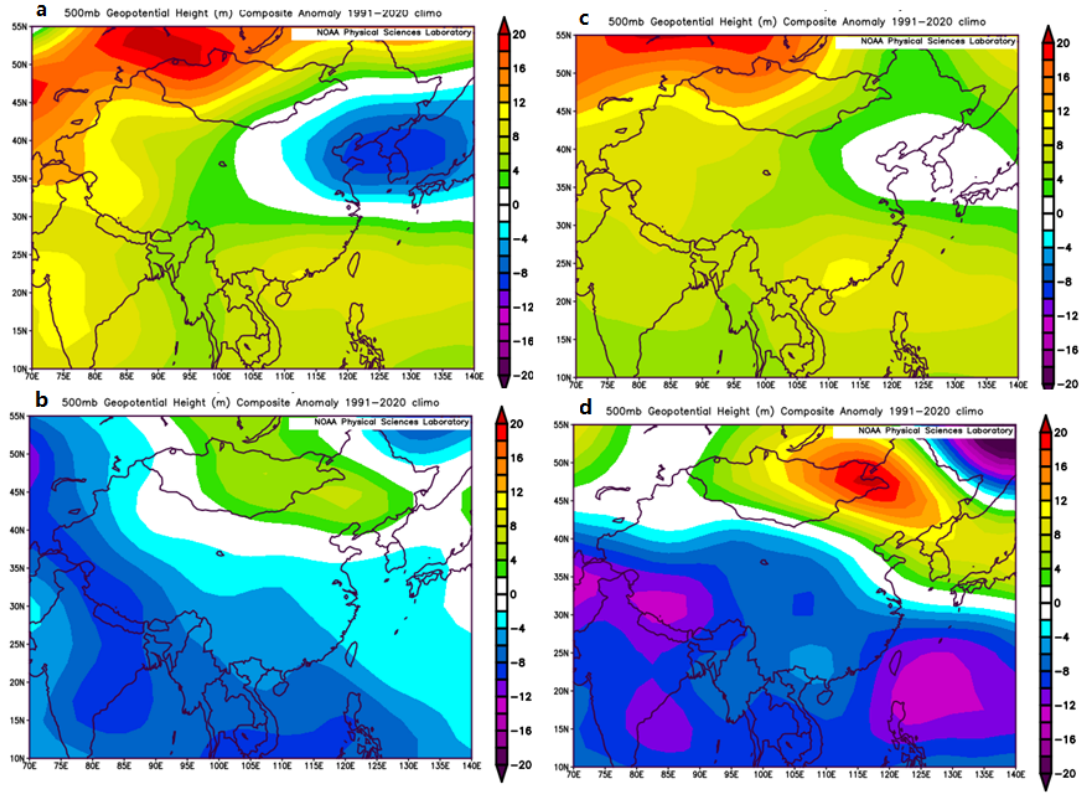

Figure S5. Composite anomalies of 500-hPa geopotential heights (ghm) in positive and negative phases of the first EOF loading (PCA1) for summer O_3 and WPSH-I1 as the departure from their respective means from 1999 to 2017. We selected those years with the positive and negative anomalies of the PCA1 and WPSHI $\geq \pm$ 1 standard deviation. **a.** Composite anomalies in the positive phase of PCA1, **b.** same as

Fig. S5a but for negative phase of PCA1, **c.** composite anomalies in the positive phase of WPSHI, **d.** same as Fig. S5c but for negative phase of WPSHI**.**

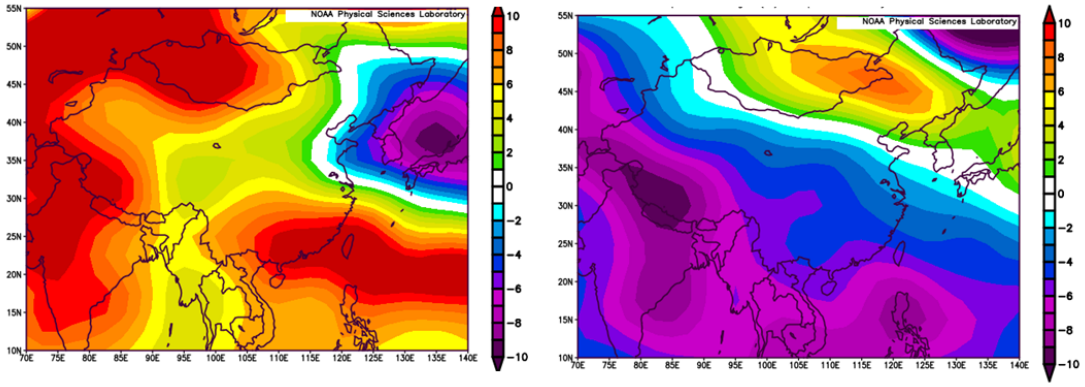

Figure S6. Composite anomalies of 500-hPa geopotential height (ghm) corresponding to **(a**) positive summer O_3 anomalies and (**b**) negative anomalies, estimated by the departure of summer mean O_3 concentrations from their mean averaged from 1980 to 2017. We selected those years with the positive and negative anomalies of O_3 concentrations $\geq \pm$ 1 standard deviation (STD, and then estimated their composite means.

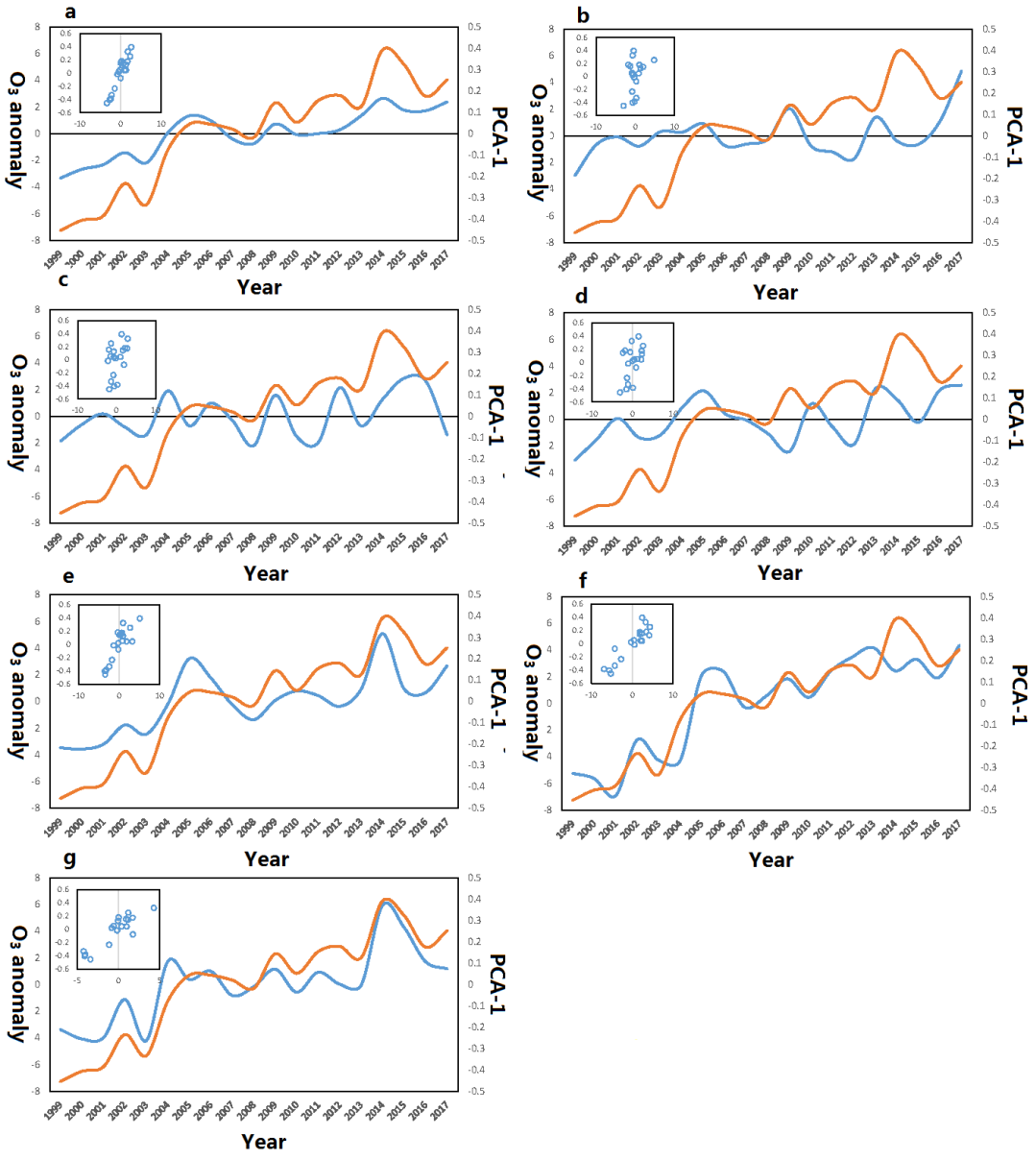

Figure S7. Annual variations of WRF-Chem simulated O_3 concentration anomalies (scaled on the left Y-axis) and PCA1 (scaled on the right Y-axis) from 1999 to 2017 averaged over the six UAs and each UA, respectively. Inset figure on the top-left is a correlation diagram between O_3 anomalies and PCA1**. (a)** Averaged over 6 UAs, **(b)** PRD, **(c)** YRD, **(d)** BTH, **(e)** CC, **(f)** CY, **(g)** MYR.

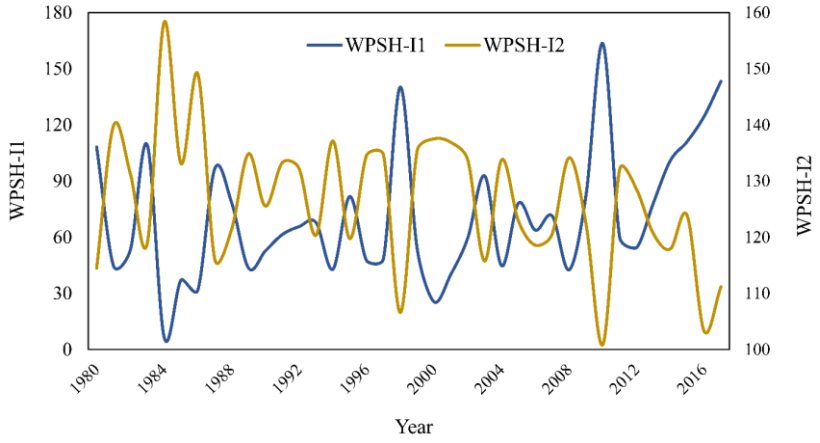

Figure S8. Annual WPSH area index (WPSH-I1) and WPSH ridge point westward shifting (WPSH-I2) from 1980 to 2017.

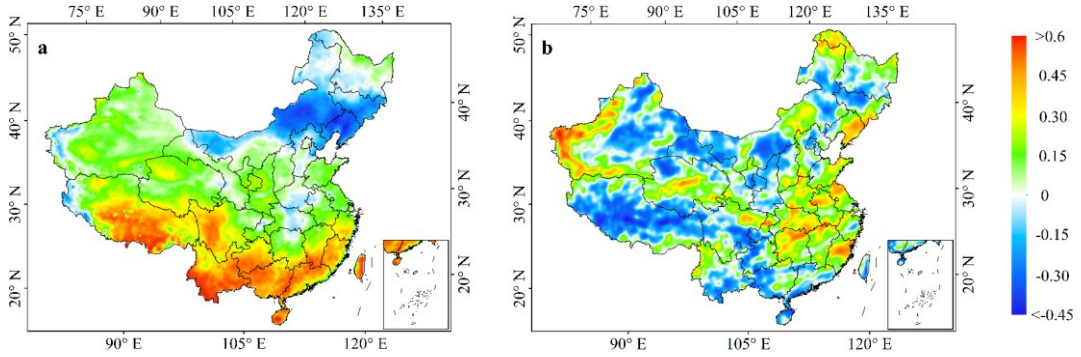

Figure S9. Correlation coefficients between summer WPSH-I1 and SAT (a) and precipitation (b) simulated under model scenario 2 (S2).

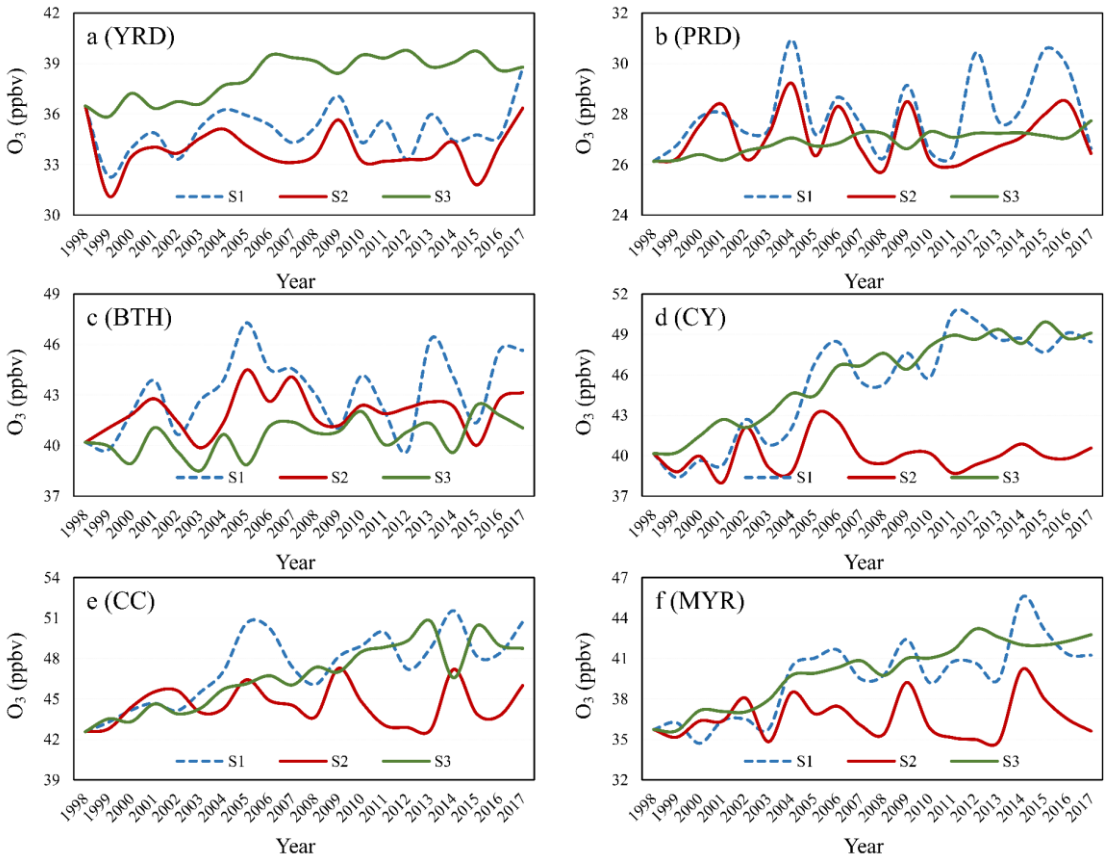

Figure S10. Annual variations of modeled summer O_3 concentrations under three model scenarios averaged over six UAs from 1998 to 2017. (a). summer O_3 concentrations averaged over YRD, S1-S3 indicate three scenarios, (b) same as Fig. S10a but for PRD, (c) same as Fig. S10a but for BTH, (d) same as Fig. S10a but for CY, (e) same as Fig. S10a but for CC, (f) same as Fig. S10a but for MYR.